

Metal-insert filters with improved characteristics

J. Bornemann and F. Arndt, Sen.Mem.I.E.E.E.

Indexing terms: Waveguides and waveguide components

Abstract: A computer-aided design is introduced for E-plane filters with single and double metal inserts within a reduced-width or increased-width waveguide section, respectively. This design achieves filter performances with high peak attenuation in a broad second stopband. The theory described includes both the higher-order mode interaction of all discontinuities and the finite thickness of the inserts. The step-wall discontinuity effect is included in the optimisation process as an additional parameter to be optimised. Ka-band (26.5–40 GHz) design examples demonstrate the good stopband attenuation behaviour of this type of filters. Moreover, this design only requires thin strips, which are very appropriate for technical realisation.

1 Introduction

All-metal inserts integrated in the E-plane of rectangular waveguides yield low-cost mass-producible millimetre-wave filters with low passband insertion loss [1-6]. However, as the filter resonators are coupled by way of evanescent fields along the inductive strips, high attenuation specifications in the second stopband are difficult to satisfy, especially by filter performances designed for passbands near the upper end of the waveguide band. This is due to unwanted direct coupling of modes along the strip sections with progressing frequency if the distance between the strips and the waveguide side walls is no longer negligible compared with the guide wavelength. To alleviate this problem, the waveguide width in the vicinity of the strips may be reduced, as has been suggested by the authors [7]. However, in Reference 7 linear taper sections are used to match the waveguide sections of different width. This requires additional mechanical efforts and thus may offset the low-cost advantage of the E-plane integrated circuit filters. Moreover, the taper sections compensate the inductive junction effects of the discontinuities, which may be advantageously utilised as an additional optimisation parameter.

In this paper, therefore, an abrupt discontinuity between the waveguide sections in question (Fig. 1) is used. This is more appropriate for a convenient mechanical construction than a smooth section. The step-wall discontinuity effect is utilised directly as an additional parameter for designing filters with high stopband attenuation. Moreover, for all designs with improved stopband attenuation, only thin strips are required which are very appropriate for production by photoetching techniques.

The abrupt step-wall discontinuity E-plane filter type may also be advantageously utilised to improve the stopband attenuation for filters with passbands near the lower

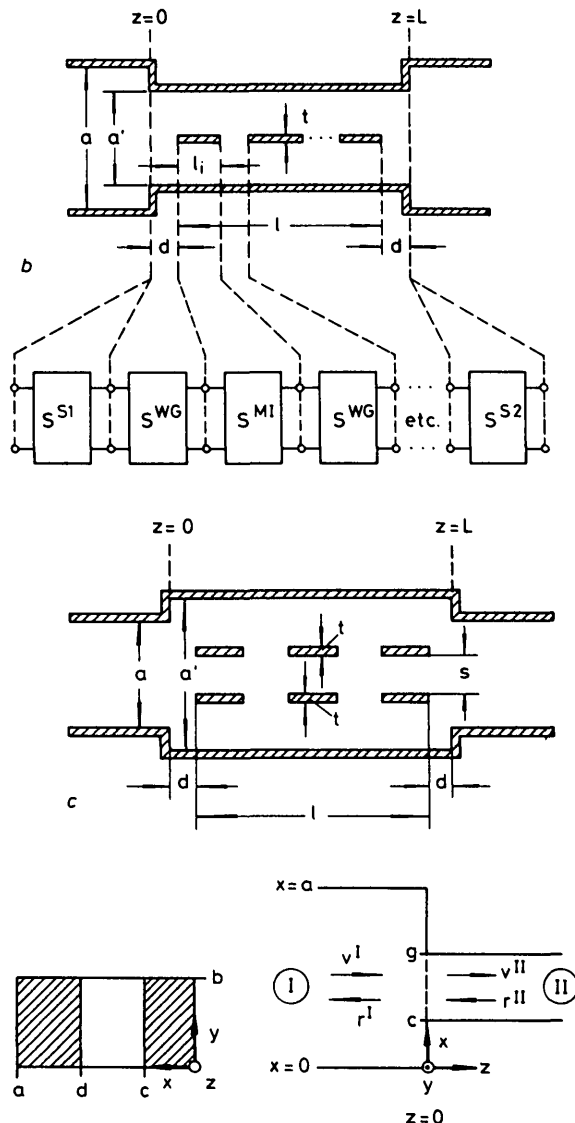
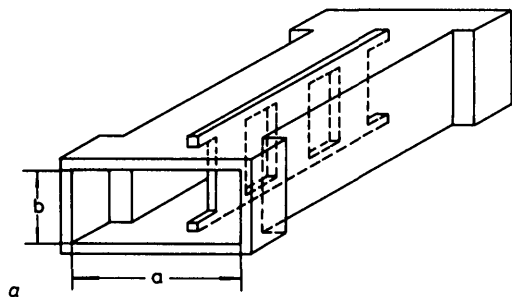


Fig. 1 E-plane metal-insert filters in waveguides with abrupt step-wall discontinuity

- a Waveguide and metal insert
- b Abruptly reduced waveguide width; high stopband attenuation filter type for passbands in the near of the upper band end of the original waveguide (width a); scattering matrices:
 S^{S1} discontinuity change in waveguide width (broad to small)
 S^{WG} homogeneous waveguide section
 S^{M1} metal-insert section of length l_i (including the discontinuities waveguide to E-plane bar section and back to waveguide)
- c Abruptly increased waveguide width; high stopband attenuation filter type for passbands in the near of the lower band end of the original waveguide (width a)
- d Configuration for the field theory treatment of the step-wall discontinuity

Paper 4450H (E12), received 7th May 1985

The authors are with the Microwave Department, University of Bremen, Kufsteiner Strasse NW1, Postfach 33 04 40, D-2800 Bremen 33, West Germany

band end of the original waveguide. For this design, however, the side-wall distance of the waveguide housing in the vicinity of the strips needs to be increased (Fig. 1c). This is due to the nonlinear relation between guide-wavelength and frequency which may be favourably influenced by a suitable reduction of the cutoff frequency of the fundamental mode within the filter resonators. High stopband attenuation over the whole waveguide band is achieved by utilising the double-insert filter type [5, 7] for the filter section within the waveguide of increased width (Fig. 1c).

As in References 3-5 and Reference 7, the design of optimised filters is based on a rigorous field expansion into incident and scattered waves at all discontinuities. This allows direct inclusion of higher-order mode coupling, finite strip thickness and the step-wall discontinuity effects in the optimisation process to make the filter performance satisfy the given specifications.

2 Theory and design

Because the field-theory treatment of the metal-insert filter structure within the length l (Figs. 1b, c) has already been described in detail in References 3 and 7, respectively, the theory in this paper may be restricted to the derivation of the scattering matrix of the step-wall discontinuity at $z = 0$ (Fig. 1d).

The fields in the subregions $i = I, II$

$$\mathbf{E}^{(i)} = \nabla \times (\mathbf{e}_z A_{hz}^{(i)}), \quad \mathbf{H}^{(i)} = \frac{j}{\omega\mu} \nabla \times \nabla \times (\mathbf{e}_z A_{hz}^{(i)}) \quad (1)$$

are derived from the z -component of the magnetic vector potential $A_{hz}^{(i)}$ which is assumed to be a sum of the eigenmodes

$$A_{hz}^{(i)} = \sum_{m=0}^M A_m^{(i)} \cdot \cos(f_m^{(i)}(x)) \cdot (v_m^{(i)} e^{-jk_{zm}^{(i)} \cdot z} + r_m^{(i)} e^{+jk_{zm}^{(i)} \cdot z}) \quad (2)$$

where

$$f_m^{(I)}(x) = k_{xm}^{(I)} x, f_m^{(II)}(x) = k_{xm}^{(II)}(x-c)$$

$$k_{zm}^{(i)} = \sqrt{(k_0^2 - (k_{xm}^{(i)})^2)}, k_0^2 = \omega^2 \mu_0 \epsilon_0$$

$$k_{xm}^{(I)} = \frac{m\pi}{a}, k_{xm}^{(II)} = \frac{m \cdot \pi}{g - c}$$

The coefficients $A_m^{(i)}$ are normalised so that the power carried by a given wave is 1 W for a wave-amplitude coefficient of $\sqrt{1 W}$

$$A_m^{(i)} = \frac{1}{k_{xm}^{(i)}} \cdot \sqrt{\frac{2\omega\mu_0}{k_{zm}^{(i)} \cdot F^{(i)}}} \quad (3)$$

with

$$F^{(I)} = ab, F^{(II)} = (g - c) \cdot b$$

By matching the tangential field components at the common interfaces across the step discontinuity at $z = 0$, as in Reference 3, the coefficients $v_m^{(i)}$ and $r_m^{(i)}$ can be related to each other. This yields the two-port scattering matrix $(\mathbf{S})^{S1}$ of the step-wall discontinuity from the wider to the narrower waveguide (at $z = 0$, Fig. 1b; at $z = L$, Fig. 1c)

$$\begin{pmatrix} r^{(I)} \\ v^{(II)} \end{pmatrix} = (\mathbf{S})^{S1} \begin{pmatrix} v^{(I)} \\ r^{(II)} \end{pmatrix} \quad (4)$$

where the coefficients of

$$(\mathbf{S})^{S1} = \begin{pmatrix} S_{11}^{S1} & S_{12}^{S1} \\ S_{21}^{S1} & S_{22}^{S1} \end{pmatrix} \quad (5)$$

are explained in Appendix 6.1.

The scattering matrix $(\mathbf{S})^{S2}$ at the step-wall discontinuity from the narrower to the wider waveguide (at $z = L$, Fig. 1b; at $z = 0$, Fig. 1c) may be obtained directly from eqn. 5 if $r^{(I)}$ and $v^{(II)}$, as well as $v^{(I)}$ and $r^{(II)}$, are interchanged. This implies that the indices in eqn. 5 are transposed

$$(\mathbf{S})^{S2} = \begin{pmatrix} S_{11}^{S2} & S_{12}^{S2} \\ S_{21}^{S2} & S_{22}^{S2} \end{pmatrix} = \begin{pmatrix} S_{22}^{S1} & S_{21}^{S1} \\ S_{12}^{S1} & S_{11}^{S1} \end{pmatrix}. \quad (6)$$

For the overall scattering matrix $(\mathbf{S})^{M1}$ of the metal-insert filter section of length l_i , including the discontinuities waveguide to E-plane bar section and back to waveguide, the reader is referred to eqn. 6 of Reference 3 concerning the single metal-insert structure (Fig. 1b), or to eqn. 7 of Reference 7 concerning the double metal-insert filter structure (Fig. 1c), respectively.

The scattering matrix of the total metal-insert filter including the two abrupt step-wall discontinuities at the beginning and end of the filter section is then calculated by directly combining the single scattering matrices (Fig. 1b), as in Reference 3. Contrary to the usual treatment with transmission matrices, this procedure preserves numerical accuracy, as the expressions contain exponential functions with only negative arguments. For completeness, the scattering coefficients for two series connected sections are given in the Appendix 6.2. The scattering matrix for more sections is found analogously using this equation iteratively.

As in References 3-5 and Reference 7, the computer-aided design of suitable filter performances is carried out by an optimising program applying the evolution strategy method. For given waveguide housing dimensions and thickness of the metallic E-plane inserts, the parameters to be optimised are the insert and the resonator lengths, as well as the distance d (Fig. 1) between the step-wall discontinuity and the first or last filter insert, respectively.

For computer optimisation, the expansion into nine eigenmodes at each discontinuity has turned out to be sufficient. The final design data are proved by expansion into 35 eigenmodes.

3 Results

The influence of the abrupt step-wall discontinuity on the behaviour of the second stopband attenuation of E-plane metal-insert filters is demonstrated in Fig. 2a, with the example of Ka-band three-resonator filters designed for a midband frequency of about 39.37 GHz, near the higher end of the Ka-band (26.5-40 GHz). The insert thickness is $t = 190 \mu\text{m}$. Curve 1 shows the insertion loss $(1/|S_{21}|)$ in decibels as a function of frequency of an optimised conventional metal-insert filter where no change in the waveguide width occurs (for design data see Table 1). The maximum attenuation in the second stopband is only about 40 dB, and the second passband already exists at about 47 GHz, due to the unwanted coupling of higher-order modes along the strip sections.

The optimised E-plane metal-insert filter with abrupt step-wall discontinuity, however, yields an attenuation of about 58 dB in the second stopband, the second passband appears at 56.5 GHz. Fig. 2b shows the detail curve of the insertion and return loss of the optimised E-plane metal-

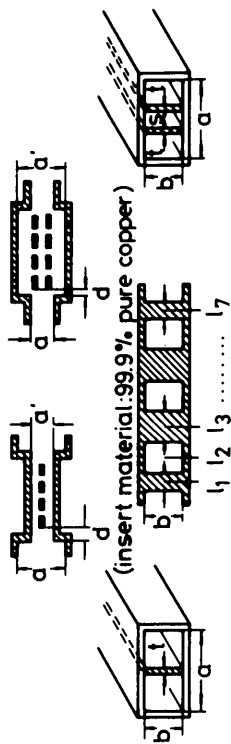


Table 1.

Frequency band for the filter design	Number of resonators	Reduced or increased waveguide width a', mm	Distance between step-wall discontinuity and filter section d, mm	Filter type†	Insert thickness t, mm	spacing s, mm	$l_1 = l_7$ mm	$l_2 = l_6$ mm	$l_3 = l_5$ mm	l_4 mm	Midband frequency GHz	3 db band width GHz	Peak attenuation in the second stopband dB	Second passband at GHz	Shown in Fig.
Ka-band	3			C	t = 0.19		2.702	2.617	6.944	2.589	39.374	0.71	40	46.5	2a, curve 1
a = 7.112 mm		5.6896	4.23	R	t = 0.19		0.963	3.903	3.014	3.916	39.375	0.71	58	56.5	2a, curve 2
b = 3.556 mm		5.6896	4.086	R	t = 0.19		0.989	3.853	3.612	3.865	39.573	0.398	64	56.6	3, curve 2
WR 28		5.6896	4.369	R	t = 0.19		0.814	4.277	3.058	4.301	37.945	0.498	62	54.6	4, curve 2
				C	t = 0.19		0.766	7.319	3.292	7.397	27	0.283	67	38.5	5a, curve 1
		8.636	4.993	I	$\frac{t=0.19}{s=1.5}$		0.718	6.215	3.218	6.236	27	0.248	81	43	5a, curve 2

† C = conventional, i.e. metal-insert filter without step-wall discontinuity, single insert

R = reduced-width single insert

I = increased-width double insert

insert filter with reduced-width waveguide. The input and output waveguide (Fig. 1b) has standard WR 28-dimensions ($a = 7.112$ mm, $b = 3.556$ mm, see Table 1),

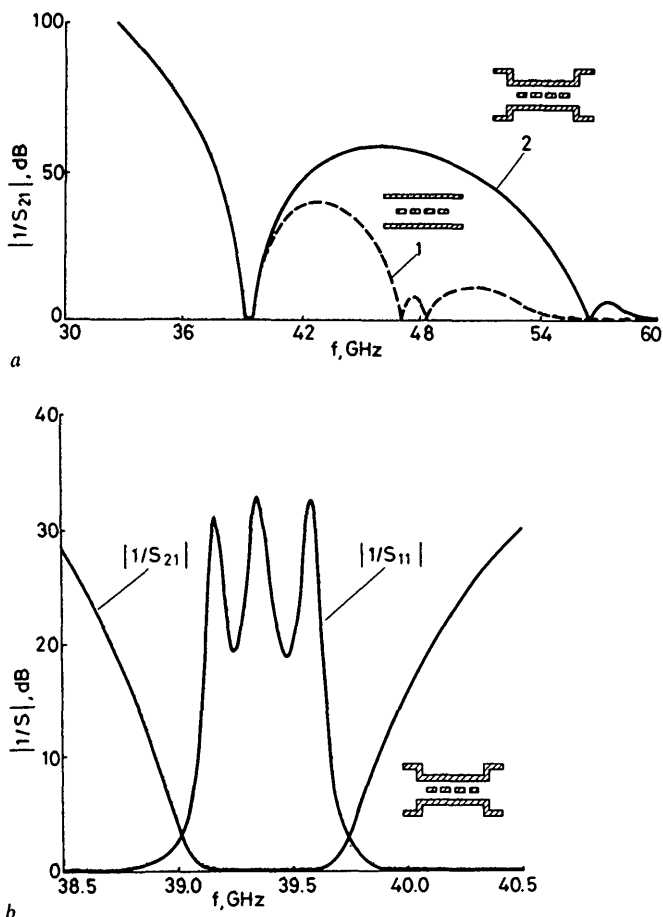


Fig. 2 Computer optimised Ka-band three-resonator metal-insert filters designed for a midband frequency of 39.37 GHz and 1.8% bandwidth

Metal-insert thickness $t = 190$ μ m (for design data see Table 1)

a Insertion loss ($1/|S_{21}|$) in decibels as a function of frequency

curve 1: conventional E-plane metal-insert filter

curve 2: E-plane metal-insert filter with abruptly reduced width waveguide step-wall discontinuity (included in the optimisation)

b Insertion loss ($1/|S_{21}|$) and return loss ($1/|S_{11}|$) in decibels as a function of frequency for the filter with step-wall discontinuity (curve 2 of Fig. 2a)

the dimension $a' = 5.689$ mm of the reduced-width section corresponds to the standard WR 22-waveguide width of the next higher-frequency band (the Q-band). The distance $d = 4.23$ mm (Fig. 1, Table 1) between the step-wall discontinuity and the metal-insert portion of the filter is also a result of the computer optimisation.

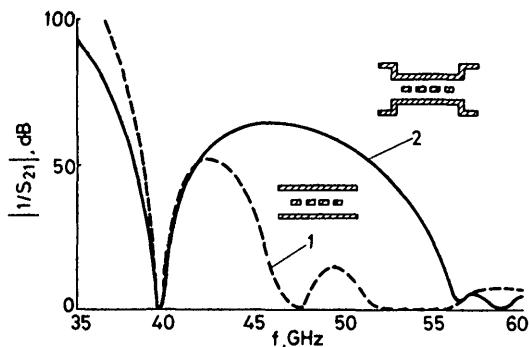


Fig. 3 Insertion loss ($1/|S_{21}|$) in decibels as a function of frequency of Ka-band three-resonator metal-insert filters with a midband frequency of 39.6 GHz and about 1% bandwidth

curve 1: conventional E-plane metal-insert filter (data from Reference 6, Fig. 13a) analysed with our method considering 35 eigenmodes. Metal-insert thickness: $t = 254$ μ m

curve 2: Computer optimised E-plane metal-insert filter with abruptly reduced width waveguide step-wall discontinuity (included in the optimisation). Metal-insert thickness: $t = 190$ μ m (for design data see Table 1)

Fig. 3 (curve 1) shows the insertion loss against frequency of a conventional three-resonator E-plane filter with inserts of thickness $t = 254$ μ m (data from Reference 6, analysed by our method considering 35 eigenmodes). In opposition to this design, the E-plane filter with abruptly reduced width waveguide, and metal inserts of $t = 190$ μ m, yields (curve 2) about 64 dB (instead of 52 dB) peak attenuation in the second stopband and a second passband at about 56 GHz (instead of 46 GHz). The optimised data of the reduced-width filter are given in Table 1.

In Fig. 4, the insertion loss of a conventional E-plane

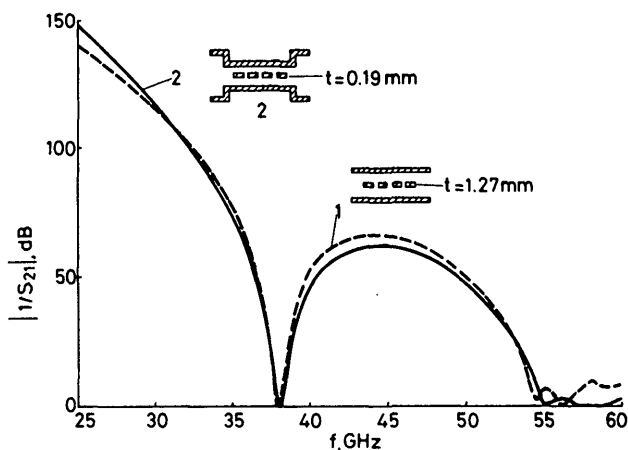


Fig. 4 Insertion loss ($1/|S_{21}|$) in decibels as a function of frequency of Ka-band three-resonators metal-insert filters with a midband frequency of 37.94 GHz and about 1.3% bandwidth

curve 1: conventional E-plane metal-insert filter (data from Reference 6, Fig. 14) analysed with our method considering 35 eigenmodes. Metal-insert thickness: $t = 1.27$ mm

curve 2: computer optimised E-plane metal-insert filter with abruptly reduced width waveguide step-wall discontinuity (included in the optimisation). Metal-insert thickness: $t = 190$ μ m (for design data see Table 1)

filter (curve 1) with thick inserts ($t = 1.27$ mm, data from Reference 6, analysed with our method considering 35 eigenmodes) is compared with that of a reduced-width E-plane filter (curve 2). Both filters yield nearly the same stopband attenuation behaviour, the reduced-width E-plane filter, however, requires only an insert thickness of $t = 190$ μ m (Table 1) which is more convenient for the physical realisation.

Fig. 5a shows the insertion loss of filters with passbands at the lower end of the Ka-band. The optimised conventional filter (curve 1) yields about 67 dB peak attenuation in the second stopband, a second passband appears already at 38.5 GHz (i.e. still within the Ka-band: 26.5–40 GHz). The corresponding values of the optimised increased-width double-metal-insert filter are 81 dB and 43 GHz; i.e. the stopband attenuation at the Ka-band end (40 GHz) is more than 45 dB. Fig. 5b shows the detail curve of the insertion and return loss of the increased-width filter (Fig. 5a, curve 2, Table 1).

4 Conclusion

A computer-aided design of optimum E-plane metal-insert filters with abrupt waveguide step-wall discontinuity has been introduced using exact field theory methods. This design achieves filter performances with high peak attenuation in a broad second stopband as may be demonstrated by comparison with conventional metal-insert filters.

According to different ranges of application, two filter types may be used. First, for passbands at the higher band end of the original waveguide, single metal-insert structures within a reduced-width waveguide alleviate the problem of higher-order mode coupling which otherwise

considerably degrades the stopband behaviour. Secondly, for passbands at the lower band end, double metal-insert

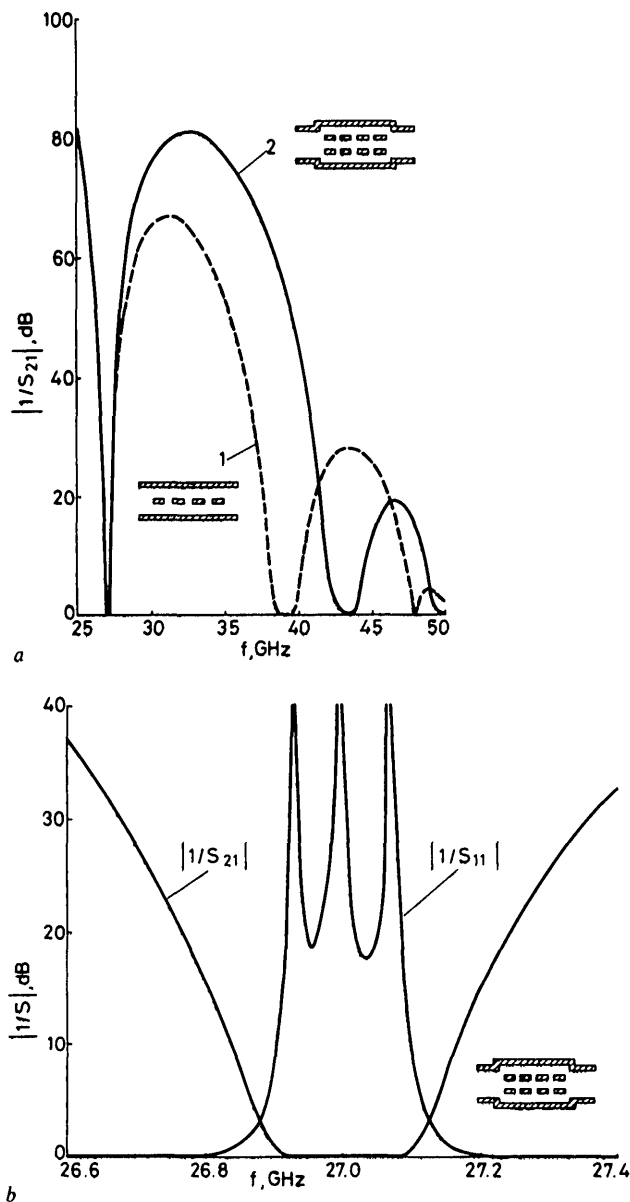


Fig. 5 Computer optimised Ka-band three-resonator metal-insert filters designed for a midband frequency of 27 GHz and about 1% bandwidth

Metal insert-thickness $t = 190 \mu\text{m}$ (for design data see Table 1)
a Insertion loss ($1/|S_{21}|$) in decibels as a function of frequency

curve 1: conventional E-plane metal-insert filter
curve 2: E-plane double metal-insert filter with abruptly increased width waveguide step-wall discontinuity (included in the optimisation)
b Insertion loss ($1/|S_{21}|$) and return loss ($1/|S_{11}|$) in decibels as a function of frequency for the filter with step-wall discontinuity (curve 2 of Fig. 5a)

structures within an increased-width waveguide, which reduces the guide wavelength of the filter resonators, yield high stopband attenuation over the whole original waveguide band.

As the step-wall discontinuity effect is utilised directly as an additional parameter to be optimised, the filters may be designed for low passband insertion losses and high attenuation levels in the second stopband, which, in addition, is much broader than the conventional metal-insert

filters. Moreover, for all improved stopband designs, only thin strips (e.g. $t = 190 \mu\text{m}$) are required, which are very appropriate for production by photoetching techniques.

5 References

- 1 TAJIMA, Y., and SAWAYAMA, Y.: 'Design and analysis of a waveguide-sandwich microwave filter', *IEEE Trans.*, 1974, **MTT-22**, pp. 839-841
- 2 KONISHI, Y., and UENAKADA, K.: 'The design of a bandpass filter with inductive strip-Planar circuit mounted in waveguide', *ibid.*, 1974, **MTT-22**, pp. 869-873
- 3 VAHLIDIECK, R., BORNEMANN, J., ARNDT, F., and GRAUERHOLZ, D.: 'Optimized waveguide E-plane metal insert filters for millimeter-wave applications', *ibid.*, 1983, **MTT-31**, pp. 65-69
- 4 VAHLIDIECK, R., BORNEMANN, J., ARNDT, F., and GRAUERHOLZ, D.: 'W-band low-insertion-loss E-plane filter', *ibid.*, 1984, **MTT-32**, pp. 133-135
- 5 BORNEMANN, J., ARNDT, F., VAHLIDIECK, R., and GRAUERHOLZ, D.: 'Double planar integrated millimeter-wave filter', 13th European Microwave Conference Nürnberg, W. Germany, September 5th-8th, 1983, pp. 168-173
- 6 SHIH, Y.C.: 'Design of waveguide E-plane filters with all-metal inserts', *IEEE Trans.*, 1984, **MTT-32**, pp. 695-704
- 7 ARNDT, F., BORNEMANN, J., VAHLIDIECK, R., and GRAUERHOLZ, D.: 'E-plane integrated circuit filters with improved stopband attenuation', *ibid.*, 1984, **MTT-32**, pp. 1391-1394

6 Appendix

6.1 Scattering coefficients in eqn. 5

$$\begin{aligned} S_{11}^1 &= 2(L_E)(W)^{-1}(L_H) - (U) \\ S_{12}^1 &= (L_E)\{(W)^{-1}[(U) - (L_H)(L_E)] + (U)\} \\ S_{21}^1 &= 2(W)^{-1}(L_H) \\ S_{22}^1 &= (W)^{-1}[(U) - (L_H)(L_E)] \end{aligned} \quad (7)$$

where $(W) = (U) + (L_H)(L_E)$ and (U) is the unit matrix.

The matrix coefficients of (L_E) are given by

$$L_{Emn} = 2 \sqrt{\frac{k_{zm}^{(1)}}{a(g-c)k_{zm}^{(2)}}} \cdot \int_c^g \sin\left(\frac{m\pi}{a}x\right) \cdot \sin\left(\frac{n\pi}{g-c}(x-c)dx\right) \quad (8)$$

when (L_H) is the transposed matrix

$$(L_H) = (L_E)^T \quad (9)$$

6.2 Scattering coefficients for two series connected structures with the scattering matrices $(S)^{(1)}$, and $(S)^{(2)}$

$$\begin{aligned} (S_{11})^{(total)} &= (S_{11})^{(1)} + (S_{12})^{(1)}[(U) - (S_{11})^{(2)} \\ &\quad \cdot (S_{22})^{(1)}]^{-1}(S_{11})^{(2)}(S_{21})^{(1)} \\ (S_{12})^{(total)} &= (S_{12})^{(1)}[(U) - (S_{11})^{(2)}(S_{22})^{(1)}]^{-1} \\ &\quad \cdot (S_{12})^{(2)} \\ (S_{21})^{(total)} &= (S_{21})^{(2)}[(U) - (S_{22})^{(1)}(S_{11})^{(2)}]^{-1} \\ &\quad \cdot (S_{21})^{(1)} \\ (S_{22})^{(total)} &= (S_{21})^{(2)}[(U) - (S_{22})^{(1)}(S_{11})^{(2)}]^{-1} \\ &\quad \cdot (S_{22})^{(1)}(S_{12})^{(2)} + (S_{22})^{(2)} \end{aligned}$$

when (U) is the unit matrix.